and numerical study, and thus confirm the applicability of the proposed formulation of partially saturated soil.

CONCLUSIONS

A new formulation of governing equation of three phase medium, consisting of solid skeleton, gas and water is proposed through a generalized fluid vector of generalized degrees of freedom in pore pressures; one for gas, other for water, in case of two degrees of freedom. This fluid vector can be further generalized to take into account the multiple degrees of freedom of pore pressures, such as mixtures of oil, water, air, natural gasses, etc. The use of the generalized fluid vector allows the apparently a simpler formulation of the governing equations resembling to that of two phase medium and thus has significant advantages when the complexity in pore filling materials are increased. Example analysis of this formation for validation is performed based on a 1D leaking test of a partially saturated soil column. In overall, the computed results are consistent with those of the previous bench marking test and numerical study, and thus confirm the applicability of the proposed formulation of partially saturated soil.

At the current status of the development of this study, the validation study is performed only for three phase medium. When the validation study is ready for the generalized fluid medium, the results will be reported elsewhere.

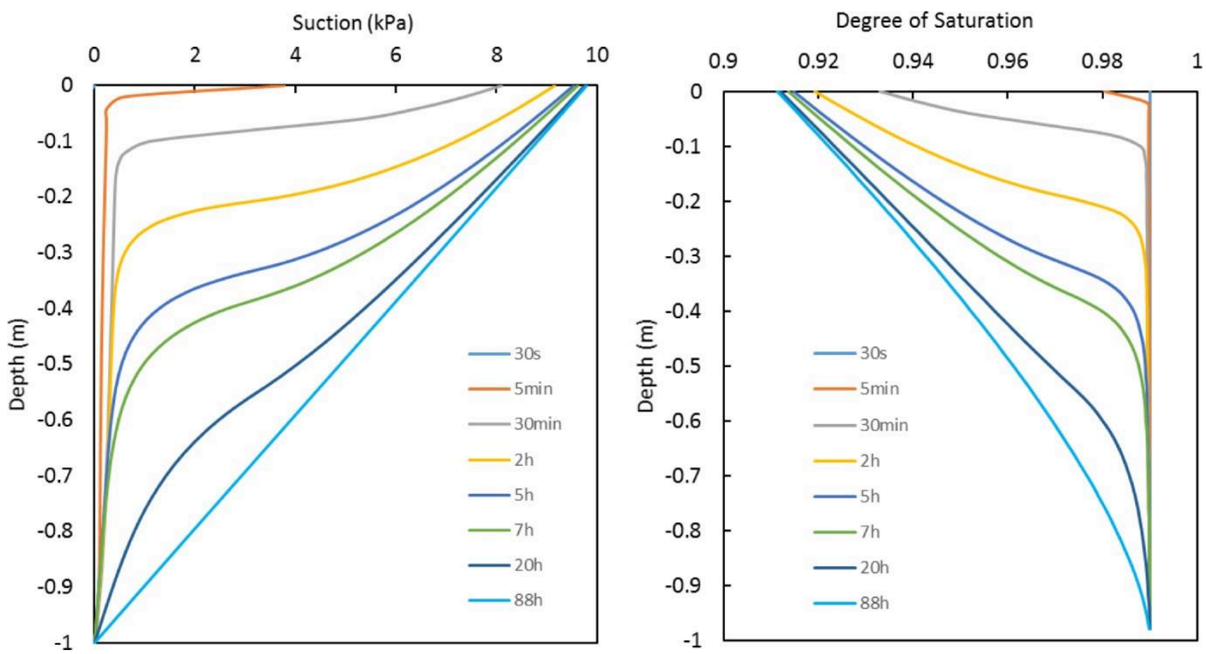

Figure 4 Computed suction and degree of saturation

REFERENCES

Borja, R. I. (2004). Cam-clay plasticity. Part v: A mathematical framework for three-phase deformation and strain localization analyses of partially saturated porous media. *Computer Methods in Applied Mechanics and Engineering, 193*, 5301-5338.

Ehlers, W., Graf, T., & Ammmann, M. (2004). Deformation and localization analysis of partially saturated soil. *Computer methods in Applied Mechanics and Engineering, 193*, 2285-2910.

Genuchten, van. (1980). A closed-form equation for predicting the hydraulic conductivity of

unsaturated soils. *Soil Science Society of America Journal, 44*, 892-898.
Liakopoulos, A. (1964). *Transient flow through unsaturated porous media.* (PhD), University of California at Berkeley.
Ohno, S., Iizuka, A., & Ohta, H. (2006). Two categories of new constitutive model derived from non-linear description of soil contractancy. *Journal of Applied Mechanics, JSCE, 9*, 407-414 (in Japanese).
Ozutsumi, O. (2003). *Numerical studies on soil-structure systems on liquefiable deposit during earthquakes.* (Doctors Dissertation), Kyoto University, Japan.
Uzuoka, R., & Borja, R. I. (2012). Dynamics of unsaturated poroelastic solids at finite strain. *International Journal for Numerical and Analytical Methods in Geomechanics, 36*, 1535-1573.
Zienkiewicz, O. C., & Bettess, P. (1982). Soils and other saturated media under transient, dynamic conditions. In Pande & Zienkiewicz (Eds.), *Soil mechanics - transient and cyclic loads* (pp. 1-16): John Wiley and Sons.

Prediction of Three-Dimensional Dynamic Soil-Pile Group Interaction in Layered Soil by Boundary Element Analysis and Seismic Cone Penetration Tests

Zhiyan Jiang, A.M.ASCE[1]; and Jeramy C. Ashlock, A.M.ASCE[2]

[1]Ph.D. Student, Dept. of Civil, Construction, and Environmental Engineering, Iowa State Univ., Ames, IA 50010, USA. E-mail: zyjiang@iastate.edu
[2]Richard L. Handy Associate Professor of Geotechnical Engineering, Dept. of Civil, Construction, and Environmental Engineering, Iowa State Univ., Ames, IA 50010, USA. E-mail: jashlock@iastate.edu

ABSTRACT

A series of full-scale dynamic vibration tests and cyclic lateral tests are to be performed on a single pipe pile and a 2×2 pile group as part of an ongoing research project. The parallelized boundary element method (BEM) code BEASSI was modified and used to predict the three-dimensional vibration response of the pile group with account of the layered soil profile including material damping and radiation damping in the viscoelastic system. The concept of the disturbed-zone model for pile groups is employed to account for pile installation effects, soil inhomogeneity, and stress- and strain-dependent modulus and damping in the near-field, while simultaneously capturing three-dimensional wave propagation and rigorously accounting for radiation damping in the far-field. To acquire accurate soil profiles as input to the analyses, a comprehensive site investigation was recently conducted, including seismic cone penetration testing with pore pressure measurement (SCPTu), standard penetration testing (SPT), and Shelby tube sampling. In the present paper, the acceleration sensor responses from SCPT tests at various depths are analyzed by the cross-correlation method to obtain shear wave velocity profiles, and the results are compared to those by the arrival time and cross-over methods, as well as empirical correlations to CPT tip resistance and sleeve friction. Material damping in the soil is also estimated from the SCPT data by the spectral ratio slope (SRS) method, which aims to minimize effects of radiation damping. The BEM program is then used with the resulting shear wave velocity profiles to calculate impedance functions in the frequency domain, which explicitly quantify the three-dimensional interaction between all the piles in the group. A general formulation based on the sub-structuring method is employed to analyze the dynamic response of pile groups using the impedance functions to obtain accelerance functions of the pile cap in vertical and coupled lateral-rocking vibration modes for validation. The findings demonstrate the accuracy and stability of the cross-correlation method for estimating shear-wave velocity from SCPT data, and an average minimum material damping ratio of 2.6% by the SRS method for the clay soils encountered. The impedance functions of the pile group indicate strong frequency-dependent dynamic soil-pile-soil interaction for the case examined. Results of this study will aid development of the proposed disturbed-zone continuum models, and provide insights into future physical pile group tests.

Keywords: soil-structure interaction; pile-groups; vibration; boundary element analysis

INTRODUCTION

Three dimensional dynamic soil-pile group interaction is a critical topic in geotechnical earthquake engineering due to the widespread use of pile foundations. In comparison to soil-pile interaction for single piles, additional complexities for pile groups arise due to sensitivities of the foundation response to the in-situ and load-induced spatial variation of the soil's shear modulus and damping profiles, influence of the relative pile and soil material properties, the 3D nature of the underlying wave propagation phenomena, interfacial contact conditions, and soil disturbance due to pile installation (Ashlock and Pak 2009). Typical methods for analysis of dynamic soil-pile interaction can be categorized as either discretized dynamic Winkler models (so called 'p-y' and 't-z' curves) (Matlock 1970; Novak 1974; Kagawa 1980; Nogami and Chen 1984) or continuum-based analytical or numerical approaches (Kuhlemeyer 1979; Kaynia and Kausel 1982).

Soil properties can vary with distance from a pile or pile group due to 1) perturbation caused by forcing a pile into the soil during driving, 2) the dependence of soil properties on the state of stress at a point, and 3) the nonlinear dependence of shear modulus and damping on shear strain. The present study applies a three-dimensional boundary element model of the piles and soil, with an inner disturbed zone surrounding the piles, and an outer semi-infinite half-space zone. The dual zones enable approximate accounts of horizontal inhomogeneity of the soil, and the multi-layered viscoelastic fundamental solutions (Pak and Guzina 1999) allow for piecewise constant vertical inhomogeneities in the soil's density, Poisson's ratio, shear modulus and material damping. The BEM code BEASSI was extended to handle the case of pile groups (Ashlock and Jiang 2017), and used for analyses of dynamic soil-pile group interaction herein. The code uses regularized boundary integral equations and allows use of singular elements (Pak and Guzina 1999) or adaptive-gradient elements (Pak and Ashlock 2007) to handle singular contact tractions inherent to mixed boundary value problems.

Soil profiles, especially the shear modulus and material damping for vibration problems, can have a significant influence on the dynamic response of pile foundations. In linear viscoelastic analyses, the soil shear modulus can be calculated using density and shear wave velocity, with the latter directly measured by in-situ or laboratory tests, or estimated by empirical correlations to SPT or CPT data. In this study, three Seismic Cone Penetration Test soundings with pore pressure measurement were conducted to measure shear wave velocities at regular intervals to a depth of 15 m. The resulting data was analyzed by the cross-correlation method in both time and frequency domains, with results compared herein to those by the arrival time and cross-over methods, as well as CPT correlations. The resulting piecewise constant shear modulus profiles were used in frequency-domain boundary element analyses to calculate impedance functions at the ground surface elevation for a 2×2 pile group. The impedance functions were then substituted into a general formulation to calculate theoretical transfer functions of directional pile-cap acceleration per unit applied force.

SEISMIC CONE PENETRATION TESTING WITH PORE PRESSURE MEASUREMENT

The experimental phase of the project includes in-situ full-scale elastodynamic vibration tests and nonlinear quasi-static cyclic-lateral tests on a 2×2 pile group. Steel pipe piles having an overall length of 9.35 m will be used, with 7.62 m (25 ft) embedded into the soil, 0.91 m (3 ft) embedded into the pile cap, and the remaining 0.81 m unembedded. The piles have an outer diameter of 21.9 cm (8.625 in.) and thickness of 0.635 cm (0.25 in.). The pile group has square layout with a pile spacing of 0.91m (3 ft) in both directions. The shear modulus, density and Poisson's ratio of the piles were assumed to be 79.37 GPa, 7850 kg/m^3 and 0.26, respectively. The pile cap is a concrete block having dimensions of 1.37 m×1.37 m×0.91 m (length × width × height). The estimated mass and polar mass moment of inertia with respect to the centroidal axis of the pile cap are 3,924 kg and 877 kg-m^2, respectively. Soil samples retrieved from the SPT split-barrel sampler were predominantly classified as glacial till clays with some small sand lenses, and the density is assumed to be uniformly 1,936.8 kg/m^3.

In general, using measured in-situ shear wave velocities is the most reliable means to evaluate the in-situ shear modulus profile of a particular soil deposit (Kramer 1996). For this purpose, the SCPTu tests were conducted at the center of the planned pile group and at the center of the single pile (Figure 1(a, b)). Tip resistance, sleeve friction and pore pressure were measured at intervals of 0.05 m depth and seismic S- and P-waves were recorded approximately every 1 m with a sampling frequency of 25,625 Hz and recording period of 100 ms. Since only a single seismic receiver is used each time, such measurements are referred as a pseudo-interval measurements. Previous studies have shown that the standard deviation of measurements is less than 1.5% of the mean value for both pseudo- and true time-interval measurements, with the latter using a pair of accelerometers simultaneously (Campanella and Stewart 1992).

The seismic wave signals are subjected to environmental and high frequency electrical noise especially at great depth, as well as low-frequency noise below 1 Hz due to DC shift. Campanella and Stewart (1992) suggested that the bulk of the signal energy occurs below 200 Hz. Transforming the signals into the frequency domain revealed that the energy in the current study is mainly distributed below 210 Hz. Therefore, the data was band-pass filtered between 1 and 210 Hz. The raw and filtered signals are plotted in Figure 1(c).

Analysis of SCPT results

Shear wave velocities

Three common methods for analyzing shear wave velocities are the arrival time method, cross-over method and cross-correlation method. In the arrival time method, the shear wave velocity is calculated as $v_s = (L_2 - L_1)/(t_2 - t_1)$, where L_1, L_2 and t_1, t_2 are travel distances and corresponding travel times from the excitation location to two observation points. However, determination of the arrival times requires subjective judgement between different potential instances of wave arrival, such as the first significant increase in acceleration amplitude. Also, the accuracy of the arrival time is affected by reading errors, especially as the signal-to-noise ratio decreases.

To overcome these shortcomings, the cross-over method was proposed. It assumes that a signal with identical amplitude and shape but opposite vibration direction can be obtained if the excitation direction is reversed. When two signals intersect after their first peak, the time is recorded as the cross-over time and differences in such time between adjacent observation points leads to an average shear wave velocity. However, the cross-over time may be shifted if the signal is perturbed near the cross-over point, which can occur due to interference between the direct shear wave arrivals in layered soils.

The cross-correlation method, which employs the entire records of the velocity or acceleration signals, was employed by Campanella and Stewart (1992). Its physical meaning is finding a time shift by which two signals have the best overall agreement. The method can be implemented in either the frequency domain or the time domain. When implemented in the frequency domain, use of the fast Fourier transform (FFT) procedure inherently assumes the finite sample record to be periodic. As a result, an unreasonable negative time shift can sometimes be identified instead of a normal positive time shift. Additionally, a windowing function may be required to avoid discontinuities at the beginning and end of the record. When implemented in the time domain, the correlation coefficient decreases as the time shift approaches ±1 recording period. However, differences in peak time shifts using the time- and frequency-domain approaches can be shown to be negligible. The frequency domain cross-correlation approach is adopted herein.

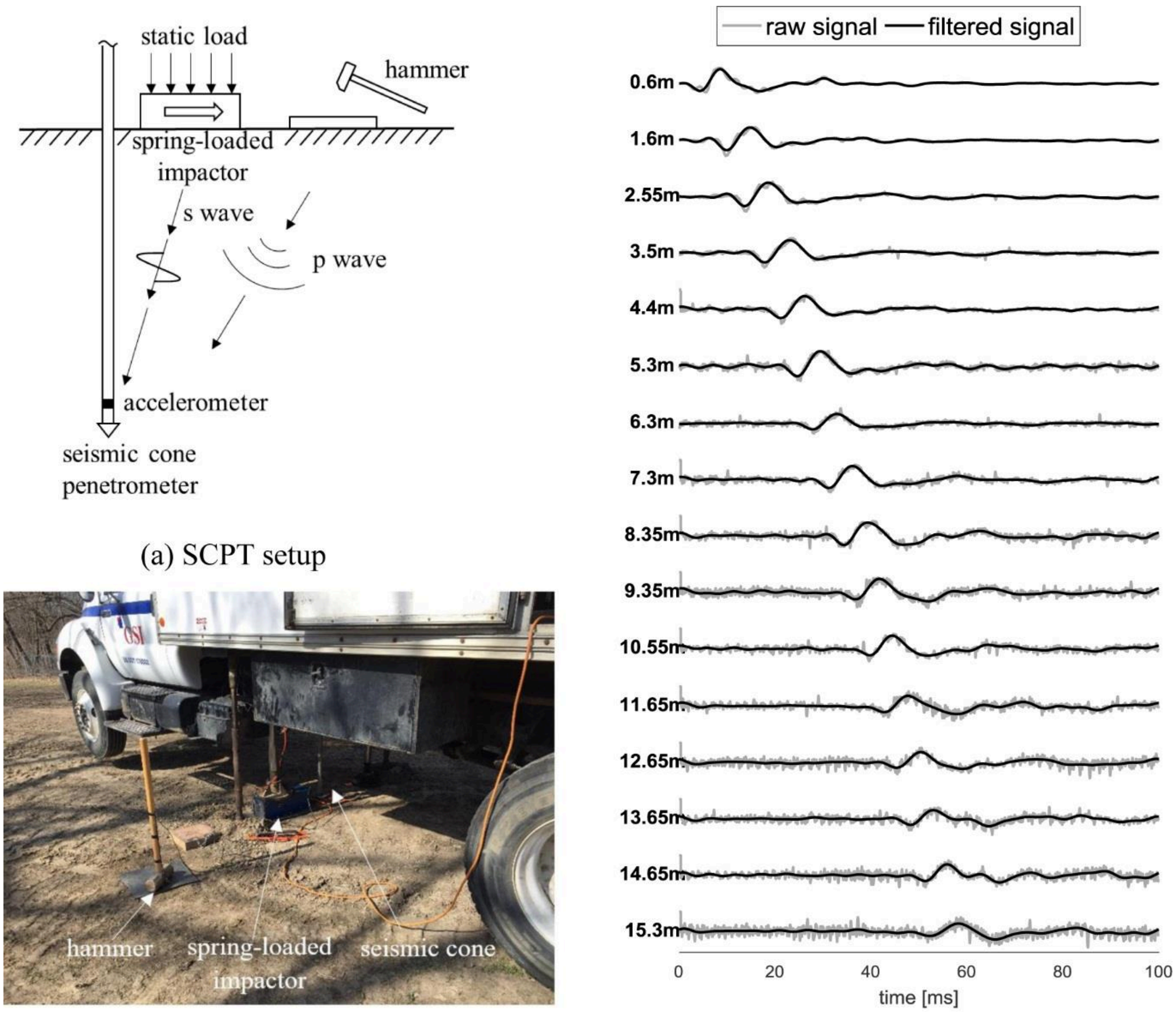

(a) SCPT setup

(b) SCPT tests

(c) raw and filtered signals for Sounding 1

Figure 1. Seismic cone penetration test setup and typical results

The SCPT data were analyzed by the three methods discussed above, and are compared in Figure 2(a), showing a reasonable agreement at depths of a few meters. However, as depth increases, the results by the arrival time method deviate from the other two methods and exhibit greater undulations. This can be explained as a result of measurement error of the pseudo-interval arrival time, which at any observation point would affect both the upper and lower neighboring layers, underestimating the velocity of one layer and simultaneously overestimating the other. All three methods show divergence with increasing depth. The increasing perturbation of the signals due to dispersion and decreasing signal-to-noise ratios with depth not only affects arrival time and cross-over time, but leads to very low normalized correlation coefficients.

In the absence of SCPT data, empirical correlations to corrected CPT tip resistance and sleeve friction are alternative options to obtain shear wave velocities. For comparison with the

SCPT results, correlations by Hegazy and Mayne (1995) for all soil types and Mayne and Rix (1995) for clay soils are shown in Figure 2(b), which reveals that both correlations conform fairly well to the SCPT results in general, although that of Mayne and Rix (1995) appears to overestimate the influence of tip resistance.

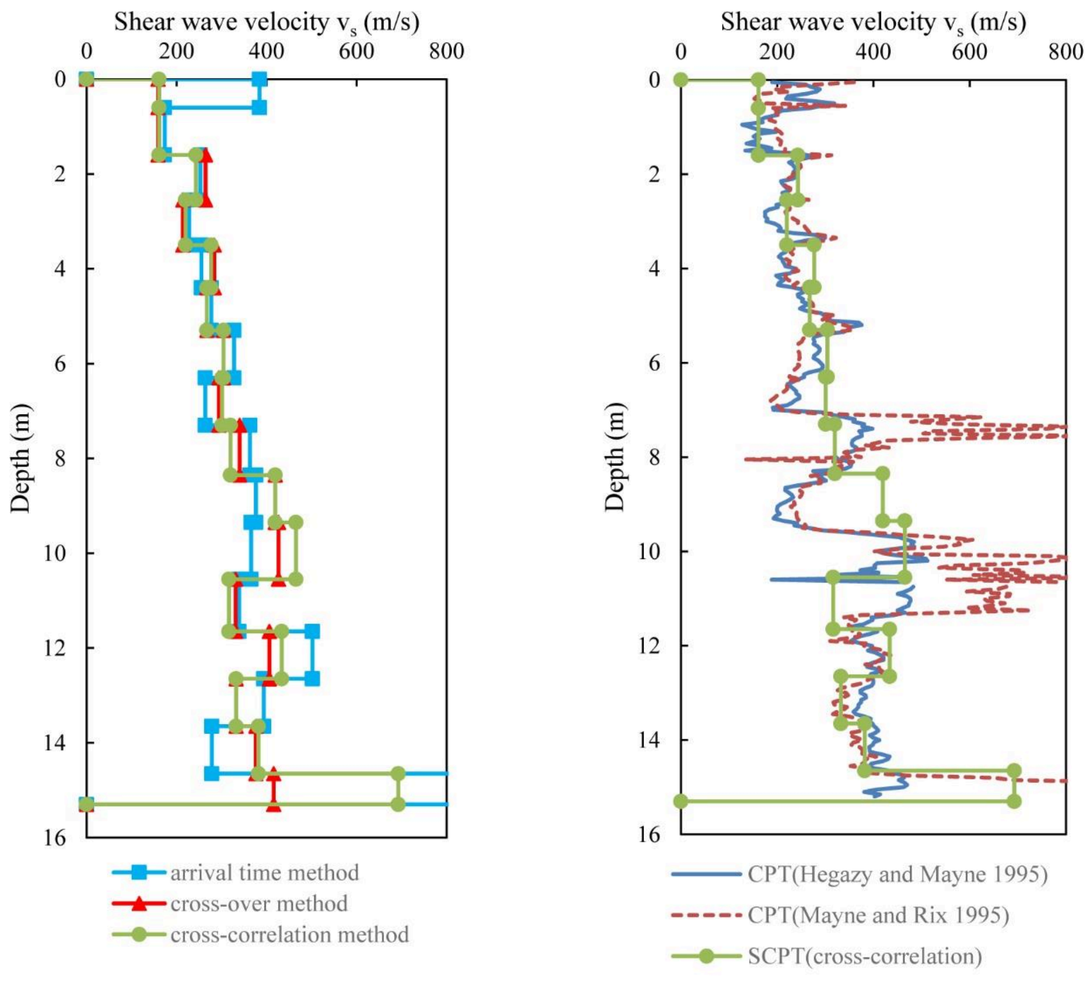

(a) V_s by SCPTu tests

(b) comparison of SCPTu tests and CPT correlations

Figure 2. Determination of shear wave velocity profile by SCPT tests and comparison to empirical correlations (CPT Sounding 1)

Minimum material damping

Although no hysteretic dissipation of energy occurs at small strain levels in the ideal case, experiments have suggested that a minimum damping ratio still exists at small strains (Hardin et al. 1999; Stokoe et al. 1999; Drnevich 2017). Efforts have thus been made to obtain material damping ratios from SCPT tests (e.g. Stewart 1992; Lutz 2005). Due to the very small vibration amplitudes in SCPT tests, for which shear strain is assumed to be less than 10^{-3}%, such material damping values can be considered to be the small-strain minimum damping.

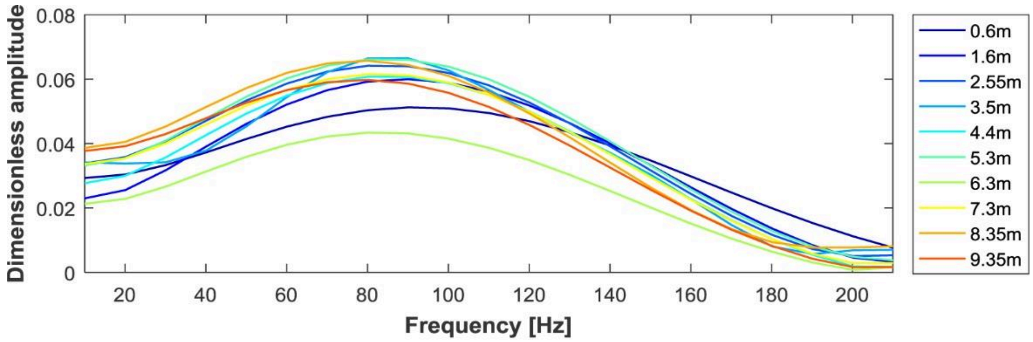

(a) SCPT signal spectrum

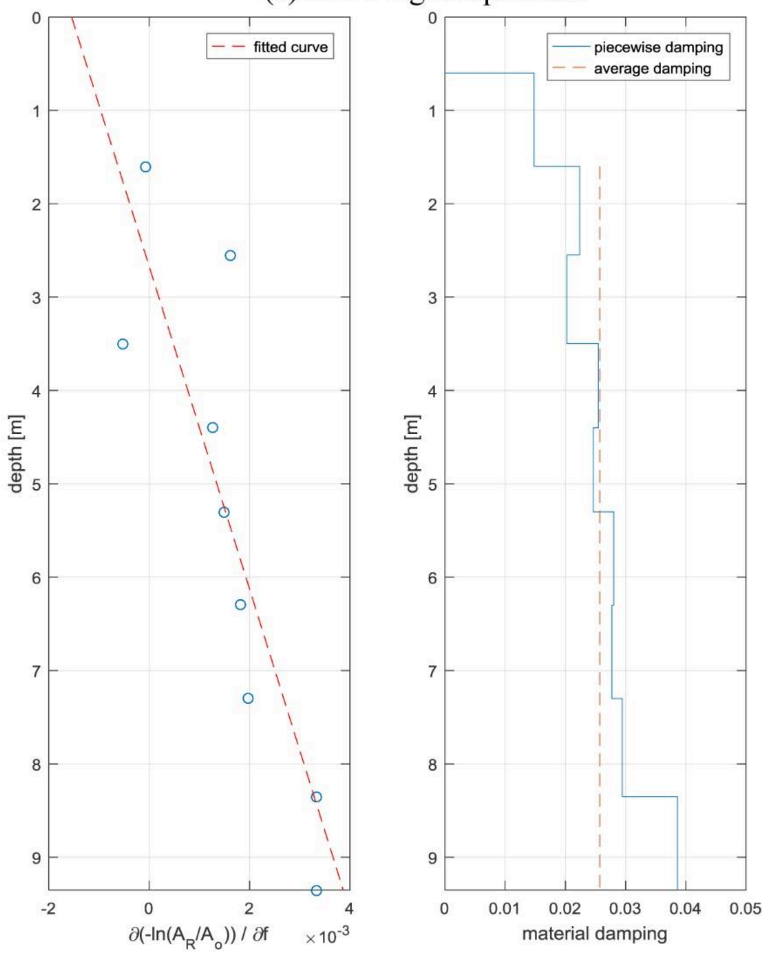

(b) fitting $\partial(-\ln A_R / A_0)/\partial f$ and result of material damping ratio

Figure 3. Application of Spectral Ratio Slope (SRS) method to determine damping at each observation depth

The spectral ratio slope (SRS) method is capable of avoiding effects of radiation damping and is believed to be a reliable method for estimating material damping from SCPT data (Stewart 1992). For simplicity, the calculation can be summarized by the equations $k = \partial^2(-\ln A_R / A_0)/(\partial f \partial R)$ and $D_s = kV_s/(2\pi)$, where A_R is the amplitude of the FFT of the sensor's signal at depth R (m) in the frequency domain, A_0 is amplitude of the FFT of a reference signal at a typical depth of 3-5 m or within a shallow surficial layer, f is frequency (Hz), V_s (m/s) is shear wave velocity of the corresponding layer, k is the slope of spectral ratio (s/m) and D_s is the material damping ratio. Shear wave signals must be windowed with a length of one cycle to obtain smooth spectral curves.

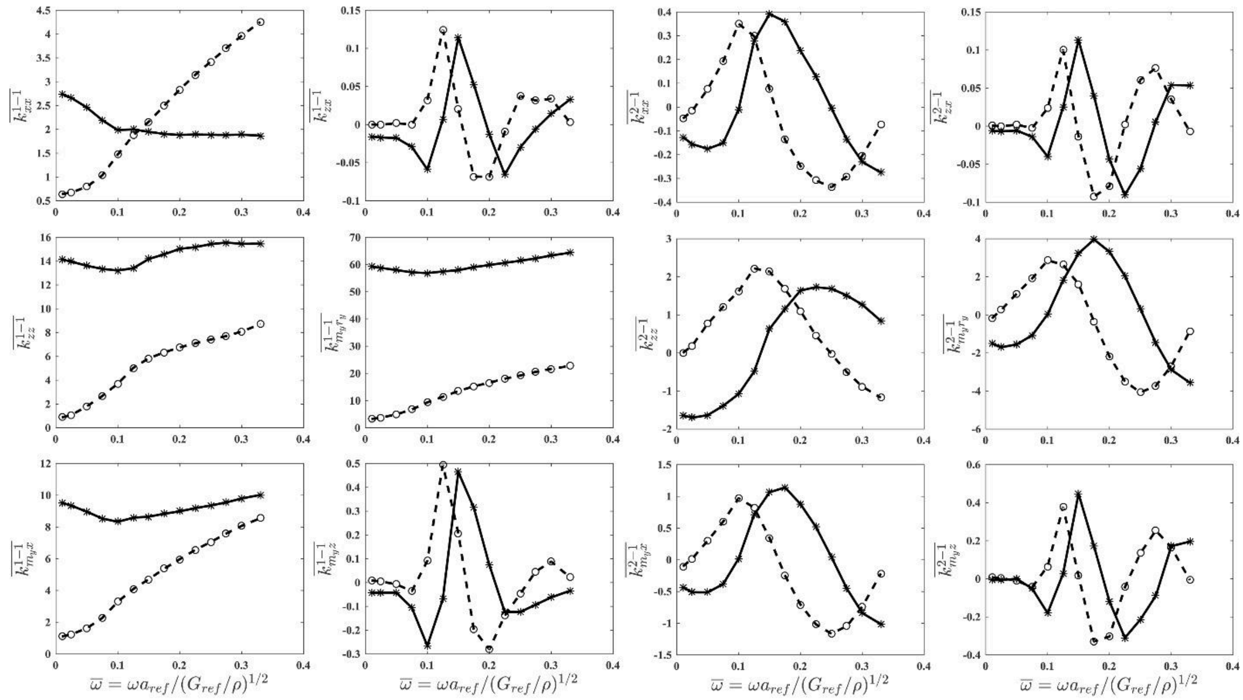

(a) Primary impedance functions in $\mathbf{K}^{1-1}$ (b) Primary impedance functions in $\mathbf{K}^{2-1}$

Figure 4. Impedance functions due to vibration of pile 1 (solid lines: real parts, dashed lines: imaginary parts)

In the present study, the signal at a depth of 0.6 m was selected as the reference, and peak FFT frequencies at all depths were around 80 Hz. After trials on multiple potential frequency ranges, the optimum frequency range for analysis was chosen as 60 to 100 Hz (Figure 3(a)), which covers most of the frequencies over which the peaks have relatively flat logarithmic ratios. The CPT tip resistance and sleeve friction suggest that there is a stiff layer between 7.05 and 8.1 m, bit it is too thin to be captured by the 1m sampling interval of the seismic tests. Points denoting $\partial(-\ln A_R / A_0)/\partial f$ from 0.6 m to 9.55 m appear to be fitted by a straight line and thus the soils are idealized as only one layer (Figure 3(b)). Averaging the piecewise damping ratios leads to an average value of 2.6%.

Poisson's ratio

The soil Poisson's ratio can be determined by 3D S- and P-wave velocities measured in in-situ tests: $v_s = \sqrt{\mu / \rho}$ and $v_p = \sqrt{(\lambda + 2\mu)/\rho}$,where v_s and v_p are secondary (shear) wave and primary (compressional) wave velocities, ρ is density and λ and μ are Lamé constants. Knowing the compressional and shear wave velocities, the Poisson's ratio ν can be determined as $\nu = 0.5(v_p^2 - 2v_s^2)/(v_p^2 - v_s^2)$. Due to insufficient P-wave velocity data in the aforementioned tests in Sounding 1, shear and primary wave profiles measured in a nearby SCPT Sounding 2 were used to estimate the Poisson's ratio profile of the clayey soil profile. The resulting Poisson's ratio values were relatively constant with depth and had an average value of 0.42 for a depth range of 0 to 10.45 m, and did not vary sharply across the ground water table at 3.66 m.

IMPEDANCE AND ACCELERANCE FUNCTIONS OF PILE GROUP

Ashlock and Jiang (2017) extended a disturbed-zone BEM model to the typical case of 2×2 pile group. In the present study, the 2×2 group of pipe piles for the experiments described above is analyzed using a disturbed zone with a radius of 1.19 m and depth of 8.81 m centered on the piles. The small strain shear modulus ($G_{\max} = \rho v_s^2$) and material damping ratio profiles in the outer half-space zone were defined using the shear modulus and damping profiles obtained from the SCPT data in the previous section. To establish the modified soil profiles inside the disturbed zone, the same ratio between inner (disturbed-zone) and outer (free-field half-space) shear moduli and the identical damping profile used in Ashlock (2006) are applied herein as a first approach.

To relate the dynamic force and moment resultants at the elevation of the ground-surface at a fixed pile i due to 3D displacements and rotations of pile j, a general elementary pile impedance submatrix can be expressed as

$$\begin{bmatrix} F_x^i \\ F_y^i \\ F_z^i \\ M_x^i \\ M_y^i \\ M_z^i \end{bmatrix} = \begin{bmatrix} k_{xx}^{i-j} & k_{xy}^{i-j} & k_{xz}^{i-j} & k_{xr_x}^{i-j} & k_{xr_y}^{i-j} & k_{xr_z}^{i-j} \\ k_{yx}^{i-j} & k_{yy}^{i-j} & k_{yz}^{i-j} & k_{yr_x}^{i-j} & k_{yr_y}^{i-j} & k_{yr_z}^{i-j} \\ k_{zx}^{i-j} & k_{zy}^{i-j} & k_{zz}^{i-j} & k_{zr_x}^{i-j} & k_{zr_y}^{i-j} & k_{zr_z}^{i-j} \\ k_{m_x x}^{i-j} & k_{m_x y}^{i-j} & k_{m_x z}^{i-j} & k_{m_x r_x}^{i-j} & k_{m_x r_y}^{i-j} & k_{m_x r_z}^{i-j} \\ k_{m_y x}^{i-j} & k_{m_y y}^{i-j} & k_{m_y z}^{i-j} & k_{m_y r_x}^{i-j} & k_{m_y r_y}^{i-j} & k_{m_y r_z}^{i-j} \\ k_{m_z x}^{i-j} & k_{m_z y}^{i-j} & k_{m_z z}^{i-j} & k_{m_z r_x}^{i-j} & k_{m_z r_y}^{i-j} & k_{m_z r_z}^{i-j} \end{bmatrix} \begin{bmatrix} U_x^j \\ U_y^j \\ U_z^j \\ \Theta_x^j \\ \Theta_y^j \\ \Theta_z^j \end{bmatrix}$$

where the first subscript denotes force or moment in the x, y, or z directions, and the second subscript denotes translation or rotation with respect to the x, y, or z axes. For the linear viscoelastic soil-pile system under consideration, the impedance relations for the four-pile group may be obtained by superposition of the individual pile impedance submatrices into a global stiffness matrix as follows:

$$\begin{bmatrix} \mathbf{F}^1 \\ \mathbf{F}^2 \\ \mathbf{F}^3 \\ \mathbf{F}^4 \end{bmatrix} = \begin{bmatrix} \mathbf{K}^{1-1} & \mathbf{K}^{1-2} & \mathbf{K}^{1-3} & \mathbf{K}^{1-4} \\ \mathbf{K}^{2-1} & \mathbf{K}^{2-2} & \mathbf{K}^{2-3} & \mathbf{K}^{2-4} \\ \mathbf{K}^{3-1} & \mathbf{K}^{3-2} & \mathbf{K}^{3-3} & \mathbf{K}^{3-4} \\ \mathbf{K}^{4-1} & \mathbf{K}^{4-2} & \mathbf{K}^{4-3} & \mathbf{K}^{4-4} \end{bmatrix} \begin{bmatrix} \mathbf{U}^1 \\ \mathbf{U}^2 \\ \mathbf{U}^3 \\ \mathbf{U}^4 \end{bmatrix} \text{ or } \mathbf{F}^i = \mathbf{K}^{i-j}\mathbf{U}^j$$

where only the impedances relevant to motion in the $x-y$ plane are included in the 3×3 $\mathbf{K}^{i-j}$ matrices. For simplicity, only a few representative entries in the elementary submatrices $\mathbf{K}^{1-1}$ and $\mathbf{K}^{2-1}$ are shown in Figure 4. The impedance functions shown for $\mathbf{K}^{1-1}$ are similar to those in the single pile case, except that $\overline{k_{zx}^{1-1}}$ and $\overline{k_{m_y z}^{1-1}}$ are no longer ideally zero as in single pile cases, because of the influence of the other three piles. For submatrix $\mathbf{K}^{2-1}$, the impedances are observed to undulate sharply with frequency, suggesting a strong frequency-dependent dynamic pile-soil-pile interaction.